Limits on anomalous trilinear gauge boson couplings from WW, WZ and $W\gamma$ production in $p\bar{p}$ collisions at $\sqrt{s} = 1.96$ TeV

D0 Collaboration

V.M. Abazov [ag], B. Abbott [br], B.S. Acharya [aa], M. Adams [av], T. Adams [at], G.D. Alexeev [ag], G. Alkhazov [ak], A. Alton [bg,1], A. Askew [at], S. Atkins [be], K. Augsten [g], C. Avila [e], F. Badaud [j], L. Bagby [au], B. Baldin [au], D.V. Bandurin [at], S. Banerjee [aa], E. Barberis [bf], P. Baringer [bc], J.F. Bartlett [au], U. Bassler [o], V. Bazterra [av], A. Bean [bc], M. Begalli [b], L. Bellantoni [au], S.B. Beri [y], G. Bernardi [n], R. Bernhard [t], I. Bertram [ao], M. Besançon [o], R. Beuselinck [ap], P.C. Bhat [au], S. Bhatia [bi], V. Bhatnagar [y], G. Blazey [aw], S. Blessing [at], K. Bloom [bj], A. Boehnlein [au], D. Boline [bo], E.E. Boos [ai], G. Borissov [ao], A. Brandt [bu], O. Brandt [u], R. Brock [bh], A. Bross [au], D. Brown [n], J. Brown [n], X.B. Bu [au], M. Buehler [au], V. Buescher [v], V. Bunichev [ai], S. Burdin [ao,2], C.P. Buszello [an], E. Camacho-Pérez [ad], B.C.K. Casey [au], H. Castilla-Valdez [ad], S. Caughron [bh], S. Chakrabarti [bo], D. Chakraborty [aw], K.M. Chan [ba], A. Chandra [bw], E. Chapon [o], G. Chen [bc], S. Chevalier-Théry [o], S.W. Cho [ac], S. Choi [ac], B. Choudhary [z], S. Cihangir [au], D. Claes [bj], J. Clutter [bc], M. Cooke [au], W.E. Cooper [au], M. Corcoran [bw], F. Couderc [o], M.-C. Cousinou [l], A. Croc [o], D. Cutts [bt], A. Das [ar], G. Davies [ap], S.J. de Jong [ae,af], E. De La Cruz-Burelo [ad], F. Déliot [o], R. Demina [bn], D. Denisov [au], S.P. Denisov [aj], S. Desai [au], C. Deterre [o], K. DeVaughan [bj], H.T. Diehl [au], M. Diesburg [au], P.F. Ding [aq], A. Dominguez [bj], A. Dubey [z], L.V. Dudko [ai], D. Duggan [bk], A. Duperrin [l], S. Dutt [y], A. Dyshkant [aw], M. Eads [bj], D. Edmunds [bh], J. Ellison [as], V.D. Elvira [au], Y. Enari [n], H. Evans [ay], A. Evdokimov [bp], V.N. Evdokimov [aj], G. Facini [bf], L. Feng [aw], T. Ferbel [bn], F. Fiedler [v], F. Filthaut [ae,af], W. Fisher [bh], H.E. Fisk [au], M. Fortner [aw], H. Fox [ao], S. Fuess [au], A. Garcia-Bellido [bn], J.A. García-González [ad], G.A. García-Guerra [ad,3], V. Gavrilov [ah], P. Gay [j], W. Geng [l,bh], D. Gerbaudo [bl], C.E. Gerber [av], Y. Gershtein [bk], G. Ginther [au,bn], G. Golovanov [ag], A. Goussiou [by], P.D. Grannis [bo], S. Greder [p], H. Greenlee [au], G. Grenier [q,r], Ph. Gris [j], J.-F. Grivaz [m], A. Grohsjean [o,4], S. Grünendahl [au], M.W. Grünewald [ab], T. Guillemin [m], G. Gutierrez [au], P. Gutierrez [br], J. Haley [bf], L. Han [d], K. Harder [aq], A. Harel [bn], J.M. Hauptman [bb], J. Hays [ap], T. Head [aq], T. Hebbeker [s], D. Hedin [aw], H. Hegab [bs], A.P. Heinson [as], U. Heintz [bt], C. Hensel [u], I. Heredia-De La Cruz [ad], K. Herner [bg], G. Hesketh [aq,6], M.D. Hildreth [ba], R. Hirosky [bx], T. Hoang [at], J.D. Hobbs [bo], B. Hoeneisen [i], J. Hogan [bw], M. Hohlfeld [v], I. Howley [bu], Z. Hubacek [g,o], V. Hynek [g], I. Iashvili [bm], Y. Ilchenko [bv], R. Illingworth [au], A.S. Ito [au], S. Jabeen [bt], M. Jaffré [m], A. Jayasinghe [br], M.S. Jeong [ac], R. Jesik [ap], P. Jiang [d], K. Johns [ar], E. Johnson [bh], M. Johnson [au], A. Jonckheere [au], P. Jonsson [ap], J. Joshi [as], A.W. Jung [au], A. Juste [al,am], E. Kajfasz [l], D. Karmanov [ai], P.A. Kasper [au], I. Katsanos [bj], R. Kehoe [bv], S. Kermiche [l], N. Khalatyan [au], A. Khanov [bs], A. Kharchilava [bm], Y.N. Kharzheev [ag], I. Kiselevich [ah], J.M. Kohli [y], A.V. Kozelov [aj], J. Kraus [bi], A. Kumar [bm], A. Kupco [h], T. Kurča [q,r], V.A. Kuzmin [ai], S. Lammers [ay], G. Landsberg [bt], P. Lebrun [q,r], H.S. Lee [ac], S.W. Lee [bb], W.M. Lee [au], X. Lei [ar], J. Lellouch [n], D. Li [n], H. Li [k], L. Li [as], Q.Z. Li [au], J.K. Lim [ac], D. Lincoln [au], J. Linnemann [bh], V.V. Lipaev [aj], R. Lipton [au], H. Liu [bv], Y. Liu [d], A. Lobodenko [ak], M. Lokajicek [h], R. Lopes de Sa [bo], H.J. Lubatti [by], R. Luna-Garcia [ad,7], A.L. Lyon [au], A.K.A. Maciel [a], R. Madar [t], R. Magaña-Villalba [ad], S. Malik [bj], V.L. Malyshev [ag], Y. Maravin [bd], J. Martínez-Ortega [ad], R. McCarthy [bo], C.L. McGivern [aq], M.M. Meijer [ae,af], A. Melnitchouk [au], D. Menezes [aw], P.G. Mercadante [c], M. Merkin [ai], A. Meyer [s], J. Meyer [u], F. Miconi [p], N.K. Mondal [aa], M. Mulhearn [bx], E. Nagy [l], M. Naimuddin [z], M. Narain [bt], R. Nayyar [ar], H.A. Neal [bg], J.P. Negret [e], P. Neustroev [ak], H.T. Nguyen [bx], T. Nunnemann [w], J. Orduna [bw], N. Osman [l], J. Osta [ba], M. Padilla [as],

A. Pal [bu], N. Parashar [az], V. Parihar [bt], S.K. Park [ac], R. Partridge [bt,5], N. Parua [ay], A. Patwa [bp], B. Penning [au],
M. Perfilov [ai], Y. Peters [u], K. Petridis [aq], G. Petrillo [bn], P. Pétroff [m], M.-A. Pleier [bp], P.L.M. Podesta-Lerma [ad,8],
V.M. Podstavkov [au], A.V. Popov [aj], M. Prewitt [bw], D. Price [ay], N. Prokopenko [aj], J. Qian [bg], A. Quadt [u],
B. Quinn [bi], M.S. Rangel [a], K. Ranjan [z], P.N. Ratoff [ao], I. Razumov [aj], P. Renkel [bv], I. Ripp-Baudot [p],
F. Rizatdinova [bs], M. Rominsky [au], A. Ross [ao], C. Royon [o], P. Rubinov [au], R. Ruchti [ba], G. Sajot [k], P. Salcido [aw],
A. Sánchez-Hernández [ad], M.P. Sanders [w], A.S. Santos [a,9], G. Savage [au], L. Sawyer [be], T. Scanlon [ap],
R.D. Schamberger [bo], Y. Scheglov [ak], H. Schellman [ax], C. Schwanenberger [aq], R. Schwienhorst [bh],
J. Sekaric [bc], H. Severini [br], E. Shabalina [u], V. Shary [o], S. Shaw [bh], A.A. Shchukin [aj], R.K. Shivpuri [z],
V. Simak [g], P. Skubic [br], P. Slattery [bn], D. Smirnov [ba], K.J. Smith [bm], G.R. Snow [bj], J. Snow [bq], S. Snyder [bp],
S. Söldner-Rembold [aq], L. Sonnenschein [s], K. Soustruznik [f], J. Stark [k], D.A. Stoyanova [aj], M. Strauss [br],
L. Suter [aq], P. Svoisky [br], M. Titov [o], V.V. Tokmenin [ag], Y.-T. Tsai [bn], K. Tschann-Grimm [bo], D. Tsybychev [bo],
B. Tuchming [o], C. Tully [bl], L. Uvarov [ak], S. Uvarov [ak], S. Uzunyan [aw], R. Van Kooten [ay], W.M. van Leeuwen [ae],
N. Varelas [av], E.W. Varnes [ar], I.A. Vasilyev [aj], P. Verdier [q,r], A.Y. Verkheev [ag], L.S. Vertogradov [ag],
M. Verzocchi [au], M. Vesterinen [aq], D. Vilanova [o], P. Vokac [g], H.D. Wahl [at], M.H.L.S. Wang [au], J. Warchol [ba],
G. Watts [by], M. Wayne [ba], J. Weichert [v], L. Welty-Rieger [ax], A. White [bu], D. Wicke [x], M.R.J. Williams [ao],
G.W. Wilson [bc], M. Wobisch [be], D.R. Wood [bf], T.R. Wyatt [aq], Y. Xie [au], R. Yamada [au], S. Yang [d], T. Yasuda [au],
Y.A. Yatsunenko [ag], W. Ye [bo], Z. Ye [au], H. Yin [au], K. Yip [bp], S.W. Youn [au], J.M. Yu [bg], J. Zennamo [bm], T. Zhao [by],
T.G. Zhao [aq], B. Zhou [bg], J. Zhu [bg], M. Zielinski [bn], D. Zieminska [ay], L. Zivkovic [bt]

[a] *LAFEX, Centro Brasileiro de Pesquisas Físicas, Rio de Janeiro, Brazil*
[b] *Universidade do Estado do Rio de Janeiro, Rio de Janeiro, Brazil*
[c] *Universidade Federal do ABC, Santo André, Brazil*
[d] *University of Science and Technology of China, Hefei, People's Republic of China*
[e] *Universidad de los Andes, Bogotá, Colombia*
[f] *Charles University, Faculty of Mathematics and Physics, Center for Particle Physics, Prague, Czech Republic*
[g] *Czech Technical University in Prague, Prague, Czech Republic*
[h] *Center for Particle Physics, Institute of Physics, Academy of Sciences of the Czech Republic, Prague, Czech Republic*
[i] *Universidad San Francisco de Quito, Quito, Ecuador*
[j] *LPC, Université Blaise Pascal, CNRS/IN2P3, Clermont, France*
[k] *LPSC, Université Joseph Fourier Grenoble 1, CNRS/IN2P3, Institut National Polytechnique de Grenoble, Grenoble, France*
[l] *CPPM, Aix-Marseille Université, CNRS/IN2P3, Marseille, France*
[m] *LAL, Université Paris-Sud, CNRS/IN2P3, Orsay, France*
[n] *LPNHE, Universités Paris VI and VII, CNRS/IN2P3, Paris, France*
[o] *CEA, Irfu, SPP, Saclay, France*
[p] *IPHC, Université de Strasbourg, CNRS/IN2P3, Strasbourg, France*
[q] *IPNL, Université Lyon 1, CNRS/IN2P3, Villeurbanne, France*
[r] *Université de Lyon, Lyon, France*
[s] *III. Physikalisches Institut A, RWTH Aachen University, Aachen, Germany*
[t] *Physikalisches Institut, Universität Freiburg, Freiburg, Germany*
[u] *II. Physikalisches Institut, Georg-August-Universität Göttingen, Göttingen, Germany*
[v] *Institut für Physik, Universität Mainz, Mainz, Germany*
[w] *Ludwig-Maximilians-Universität München, München, Germany*
[x] *Fachbereich Physik, Bergische Universität Wuppertal, Wuppertal, Germany*
[y] *Panjab University, Chandigarh, India*
[z] *Delhi University, Delhi, India*
[aa] *Tata Institute of Fundamental Research, Mumbai, India*
[ab] *University College Dublin, Dublin, Ireland*
[ac] *Korea Detector Laboratory, Korea University, Seoul, Republic of Korea*
[ad] *CINVESTAV, Mexico City, Mexico*
[ae] *Nikhef, Science Park, Amsterdam, The Netherlands*
[af] *Radboud University Nijmegen, Nijmegen, The Netherlands*
[ag] *Joint Institute for Nuclear Research, Dubna, Russia*
[ah] *Institute for Theoretical and Experimental Physics, Moscow, Russia*
[ai] *Moscow State University, Moscow, Russia*
[aj] *Institute for High Energy Physics, Protvino, Russia*
[ak] *Petersburg Nuclear Physics Institute, St. Petersburg, Russia*
[al] *Institució Catalana de Recerca i Estudis Avançats (ICREA), Spain*
[am] *Institut de Física d'Altes Energies (IFAE), Barcelona, Spain*
[an] *Uppsala University, Uppsala, Sweden*
[ao] *Lancaster University, Lancaster LA1 4YB, United Kingdom*
[ap] *Imperial College London, London SW7 2AZ, United Kingdom*
[aq] *The University of Manchester, Manchester M13 9PL, United Kingdom*
[ar] *University of Arizona, Tucson, AZ 85721, USA*
[as] *University of California Riverside, Riverside, CA 92521, USA*
[at] *Florida State University, Tallahassee, FL 32306, USA*
[au] *Fermi National Accelerator Laboratory, Batavia, IL 60510, USA*
[av] *University of Illinois at Chicago, Chicago, IL 60607, USA*
[aw] *Northern Illinois University, DeKalb, IL 60115, USA*
[ax] *Northwestern University, Evanston, IL 60208, USA*
[ay] *Indiana University, Bloomington, IN 47405, USA*

az *Purdue University Calumet, Hammond, IN 46323, USA*
ba *University of Notre Dame, Notre Dame, IN 46556, USA*
bb *Iowa State University, Ames, IA 50011, USA*
bc *University of Kansas, Lawrence, KS 66045, USA*
bd *Kansas State University, Manhattan, KS 66506, USA*
be *Louisiana Tech University, Ruston, LA 71272, USA*
bf *Northeastern University, Boston, MA 02115, USA*
bg *University of Michigan, Ann Arbor, MI 48109, USA*
bh *Michigan State University, East Lansing, MI 48824, USA*
bi *University of Mississippi, University, MS 38677, USA*
bj *University of Nebraska, Lincoln, NE 68588, USA*
bk *Rutgers University, Piscataway, NJ 08855, USA*
bl *Princeton University, Princeton, NJ 08544, USA*
bm *State University of New York, Buffalo, NY 14260, USA*
bn *University of Rochester, Rochester, NY 14627, USA*
bo *State University of New York, Stony Brook, NY 11794, USA*
bp *Brookhaven National Laboratory, Upton, NY 11973, USA*
bq *Langston University, Langston, OK 73050, USA*
br *University of Oklahoma, Norman, OK 73019, USA*
bs *Oklahoma State University, Stillwater, OK 74078, USA*
bt *Brown University, Providence, RI 02912, USA*
bu *University of Texas, Arlington, TX 76019, USA*
bv *Southern Methodist University, Dallas, TX 75275, USA*
bw *Rice University, Houston, TX 77005, USA*
bx *University of Virginia, Charlottesville, VA 22904, USA*
by *University of Washington, Seattle, WA 98195, USA*

A R T I C L E   I N F O

A B S T R A C T

We present searches for the anomalous γWW and ZWW trilinear gauge boson couplings from WW and WZ production using lepton plus dijet final states and a combination with results from $W\gamma$, WW, and WZ production with leptonic final states. The analyzed data correspond to up to 8.6 fb^{-1} of integrated luminosity collected by the D0 detector in $p\bar{p}$ collisions at $\sqrt{s} = 1.96$ TeV. We set the most stringent limits at a hadron collider to date assuming two different relations between the anomalous coupling parameters $\Delta\kappa_\gamma$, λ, and Δg_1^Z for a cutoff energy scale $\Lambda = 2$ TeV. The combined 68% C.L. limits are $-0.057 < \Delta\kappa_\gamma < 0.154$, $-0.015 < \lambda < 0.028$, and $-0.008 < \Delta g_1^Z < 0.054$ for the LEP parameterization, and $-0.007 < \Delta\kappa < 0.081$ and $-0.017 < \lambda < 0.028$ for the equal couplings parameterization. We also present the most stringent limits of the W boson magnetic dipole and electric quadrupole moments.

In the standard model (SM), the neutral vector bosons, γ and Z, do not interact among themselves, while the charged vector bosons, $W^\pm$, couple with the neutral ones and among themselves through trilinear and quartic gauge interactions. The most general γWW and ZWW interactions can be described using a Lorentz invariant effective Lagrangian that contains fourteen dimensionless couplings, seven each for γWW and ZWW [1,2]. Assuming C (charge) and P (parity) conservation and electromagnetic gauge invariance, i.e. $g_1^\gamma = 1$ where g_1^γ is the C and P conserving trilinear gauge boson coupling, reduces the number of independent couplings to five, and the Lagrangian terms take the form:

$$\frac{\mathcal{L}_{VWW}}{g_{VWW}} = ig_1^V \left(W_{\mu\nu}^\dagger W^\mu V^\nu - W_\mu^\dagger V_\nu W^{\mu\nu} \right)$$
$$+ i\kappa_V W_\mu^\dagger W_\nu V^{\mu\nu} + i\frac{\lambda_V}{M_W^2} W_{\lambda\mu}^\dagger W_\nu^\mu V^{\nu\lambda}, \qquad (1)$$

where W^μ denotes the W boson field, V^μ is either the photon ($V = \gamma$) or the Z boson ($V = Z$) field, $W_{\mu\nu} = \partial_\mu W_\nu - \partial_\nu W_\mu$, $V_{\mu\nu} = \partial_\mu V_\nu - \partial_\nu V_\mu$, and M_W is the mass of the W boson. The global coupling parameters g_{VWW} are $g_{\gamma WW} = -e$ and $g_{ZWW} = -e\cot\theta_W$, as in the SM, where e and θ_W are the magnitude of the electron charge and the weak mixing angle, respectively. In the SM, the five remaining couplings are $\lambda_\gamma = \lambda_Z = 0$ and $g_1^Z = \kappa_\gamma = \kappa_Z = 1$. Any deviation of these couplings from their predicted SM values would be an indication for new physics [3] and could provide information on a mechanism for electroweak symmetry breaking. These deviations are denoted as the anomalous trilinear gauge couplings (ATGCs) $\Delta\kappa_V$ and Δg_1^Z defined as $\kappa_V - 1$ and $g_1^Z - 1$, respectively. The W boson magnetic dipole moment, μ_W, and electric quadrupole moment, q_W, are related to the coupling parameters by:

$$\mu_W = \frac{e}{2M_W}(1 + \kappa_\gamma + \lambda_\gamma), \qquad q_W = -\frac{e}{M_W^2}(\kappa_\gamma - \lambda_\gamma). \qquad (2)$$

If the coupling parameters have non-SM values, the amplitudes for gauge boson pair production may grow with energy, eventually violating tree-level unitarity. Unitarity violation can be controlled by parameterizing the ATGCs as dipole form factors with a cutoff energy scale, Λ. The ATGCs then take the form $a(\hat{s}) = a_0/(1 + \hat{s}/\Lambda^2)^2$ in which $\sqrt{\hat{s}}$ is the center-of-mass energy of the

1 Visitor from Augustana College, Sioux Falls, SD, USA.
2 Visitor from The University of Liverpool, Liverpool, UK.
3 Visitor from UPIITA-IPN, Mexico City, Mexico.
4 Visitor from DESY, Hamburg, Germany.
5 Visitor from SLAC, Menlo Park, CA, USA.
6 Visitor from University College London, London, UK.
7 Visitor from Centro de Investigacion en Computacion, IPN, Mexico City, Mexico.
8 Visitor from ECFM, Universidad Autonoma de Sinaloa, Culiacán, Mexico.
9 Visitor from Universidade Estadual Paulista, São Paulo, Brazil.

colliding partons and a_0 is the coupling value in the limit $\hat{s} \to 0$.[10] The quantity Λ is interpreted as the energy scale where the new phenomenon responsible for the ATGCs is directly observable. At the Tevatron the cutoff scale $\Lambda = 2$ TeV is chosen such that the unitarity limits are close to, but not tighter than, the coupling limits set by data.

We assume two scenarios for studying the ATGCs. The parameterization used by the LEP experiments [4] (we refer to this as the LEP parameterization) assumes the following relation between the ATGCs:

$$\Delta \kappa_Z = \Delta g_1^Z - \Delta \kappa_\gamma \cdot \tan^2 \theta_W, \quad \text{and} \quad \lambda_Z = \lambda_\gamma = \lambda, \quad (3)$$

which is a consequence of requiring the effective low-energy Lagrangian [5], constructed from the electroweak gauge bosons and the Higgs doublet field, to be invariant under a $SU(2)_L \times U(1)_Y$ gauge symmetry. In the equal couplings scenario [2], the γWW and the ZWW couplings are set equal to each other, which is a consequence of any model that includes mixing of neutral gauge bosons. These couplings are sensitive to interference effects between the photon and Z-exchange diagrams in WW production. Electromagnetic gauge invariance requires that $\Delta g_1^Z = \Delta g_1^\gamma = 0$ and

$$\Delta \kappa_Z = \Delta \kappa_\gamma = \Delta \kappa \quad \text{and} \quad \lambda_Z = \lambda_\gamma = \lambda. \quad (4)$$

In the following analyses, we consider these two scenarios and set limits on $\Delta \kappa_\gamma$, λ, and Δg_1^Z assuming the relations above with $\Lambda = 2$ TeV.

Previously published combined limits on ATGCs at the Tevatron come from the D0 Collaboration from a combination of $W\gamma \to \ell\nu\gamma$, $WW \to \ell\nu\ell\nu$, $WW + WZ \to \ell\nu jj$ and $WZ \to \ell\nu ee$ channels (j is a jet, ℓ is an electron, e, or muon, μ, and ν is a neutrino) with integrated luminosity, $\mathcal{L}$, up to 100 pb^{-1} [6], and from the CDF Collaboration from a combination of $WW + WZ \to \ell\nu jj$ and $W\gamma \to \ell\nu\gamma$ channels with $\mathcal{L} \approx 350$ pb^{-1} [7]. The LEP experiments published ATGC limits analyzing primarily WW production [8–11] while the CMS and ATLAS experiments at the LHC pp collider have published limits on $\gamma WW/ZWW$ couplings from individual $W\gamma$, WW and WZ final states [12,13].

In this Letter, we measure the coupling parameters at the γWW and ZWW trilinear vertices through the study of gauge boson pair production. The WW final state is sensitive to both the γWW and ZWW couplings. On the other hand, the WZ and $W\gamma$ final states each only have sensitivity to the ZWW and γWW coupling, respectively. First, we present new 4.3 fb^{-1} ATGC results from $WW + WZ \to \ell\nu jj$ production and new 8.6 fb^{-1} ATGC results from $WZ \to \ell\nu\ell\ell$ production where a W boson decays leptonically and the other boson decays into a dijet or dilepton pair. These results are then combined with previously published ATGC measurements from $W\gamma \to \ell\nu\gamma$ [14,15], $WW \to \ell\nu\ell\nu$ [16] and $WW + WZ \to \ell\nu jj$ [17] production which analyzed 4.9 fb^{-1}, 1.0 fb^{-1} and 1.1 fb^{-1} of integrated luminosity, respectively. The 1.1 fb^{-1} of integrated luminosity used in the previous analysis of $\ell\nu jj$ final states is independent from the data analyzed in this Letter. Each measurement used data collected by the D0 detector [18] from $p\bar{p}$ collisions at $\sqrt{s} = 1.96$ TeV delivered by the Fermilab Tevatron Collider.

The D0 detector is a general purpose collider detector consisting of a central tracking system located within a 2 T superconducting solenoidal magnet, a hermetic liquid-argon and uranium calorimeter [19], and an outer muon system [20] surrounding 1.8 T iron toroids. Details on the reconstruction and identification criteria for electrons, muons, jets, and missing transverse energy, $\not{E}_T$, and for selection of $W\gamma \to \ell\nu\gamma$, $WW \to \ell\nu\ell\nu$, $WW + WZ \to \ell\nu jj$, and $WZ \to \ell\nu\ell\ell$ final states can be found elsewhere [14–17,21,22].

The analysis of $WW + WZ \to \ell\nu jj$ final states extends a previous D0 analysis of 4.3 fb^{-1} of integrated luminosity which measured the WW and WZ cross sections [21]. To select $WW + WZ \to \ell\nu jj$ candidates, we require a single reconstructed electron (muon) with transverse momentum $p_T > 15$ (20) GeV and pseudorapidity $|\eta| < 1.1$ (2.0),[11] $\not{E}_T > 20$ GeV, two or three reconstructed jets with $p_T > 20$ GeV and $|\eta| < 2.5$, and the W transverse mass [23], $M_T^{\ell\nu}$ (GeV) $> 40 - 0.5\not{E}_T$. The reconstructed transverse momentum of the two most energetic jets (p_T^{jj}) of selected $\ell\nu jj$ candidates is used to search for ATGCs. In order to maximize the sensitivity to ATGCs, only candidate events within a dijet invariant mass in the range of $55 < M_{jj} < 110$ GeV are studied.

The ATGC analysis of $WZ \to \ell\nu\ell\ell$ final states builds upon a previous D0 measurement of the WZ cross section [22] with 8.6 fb^{-1} of integrated luminosity and uses the reconstructed transverse momentum of the two leptons ($p_T^{\ell\ell}$) originating from the Z boson. To select $WZ \to \ell\nu\ell\ell$ candidates, we require $\not{E}_T > 20$ GeV, at least two oppositely charged electrons (muons) with $|\eta| < 3.0$ (2.0), $p_T^1 > 20$ (15) GeV and $p_T^2 > 15$ (10) GeV, and with an invariant mass $60 < M_{\ell\ell} < 120$ GeV. An additional electron or muon is required to have $p_T > 15$ GeV. In the case of three like-flavor leptons, the oppositely charged lepton pair with $M_{\ell\ell}$ more consistent with the Z boson mass is assigned to the Z decay provided that at least one of the two leptons has $p_T > 25$ GeV. Otherwise the event is rejected.

The SM $WW + WZ \to \ell\nu jj$ and $WZ \to \ell\nu\ell\ell$ production and most of the other background processes are modeled using Monte Carlo (MC) simulation. In $\ell\nu jj$ production the dominant background is due to the production of a vector boson ($V = W, Z$) in association with jets from light or heavy flavor parton production followed by the production of singe top quarks or top quark pairs. These backgrounds are modeled by MC simulation, while the multijet background is determined from data. In $\ell\nu\ell\ell$ production the dominant $Z/\gamma^* \to \ell\ell$, ZZ and $Z\gamma$ backgrounds are modeled with MC. Detailed information about the background modeling can be found elsewhere [21,22]. The SM $WW + WZ \to \ell\nu jj$ and $WZ \to \ell\nu\ell\ell$ events are generated with PYTHIA [24] using CTEQ6L1 parton distribution functions (PDFs) [25]. PYTHIA is a leading order (LO) generator, therefore we correct the event kinematics and the acceptance of $\ell\nu jj$ events for next-to-LO (NLO) and resummation effects. To derive this correction we use MC@NLO [26] with CTEQ6.1M PDFs interfaced to HERWIG [27] for parton showering and hadronization. Comparing PYTHIA to MC@NLO kinematics at the generator level after final state radiation, we parameterize a two-dimensional correction matrix in the p_T of the diboson system and that of the highest-p_T boson, and use it to reweight the PYTHIA $\ell\nu jj$ events. The event yields for the $WW \to \ell\nu jj$ and $WZ \to \ell\nu jj$ production are normalized to the SM NLO cross sections of $\sigma(WW) = 11.7 \pm 0.8$ pb and $\sigma(WZ) = 3.5 \pm 0.3$ pb calculated with MCFM [28] using MSTW2008 PDFs. The above procedure is designed to give NLO predictions at the detector level for the SM contributions to the diboson processes. The $WZ \to \ell\nu\ell\ell$ events are also generated using PYTHIA with CTEQ6L1 PDFs and thus also need to be corrected as a function of diboson p_T to

---

[10] Limits on anomalous couplings presented in this Letter are given as the low energy limits of the couplings.

[11] D0 uses a coordinate system with the z axis running along the proton beam axis. The angles θ and ϕ are the polar and azimuthal angles, respectively. Pseudorapidity is defined as $\eta = -\ln[\tan(\theta/2)]$, where θ is measured with respect to the proton beam direction.

match predictions from the NLO event generator POWHEG [29]. The event yields for $WZ \to \ell\nu\ell\ell$ production are normalized to the SM NLO cross section of $\sigma(WZ) = 3.2 \pm 0.1$ pb calculated for the Z boson invariant mass range of $60 < M_Z < 120$ GeV with MCFM and MSTW2008 PDFs.

All MC events undergo a GEANT-based [30] detector simulation and are reconstructed using the same algorithms as used for D0 data. The effect of multiple $p\bar{p}$ interactions is included by overlaying data events from random beam crossings on simulated events. We apply corrections to the MC to account for differences with data in reconstruction and identification efficiencies of leptons and jets. Trigger efficiencies measured in data are applied to MC. The instantaneous luminosity profile and z distribution of the $p\bar{p}$ interaction vertex of each MC sample are adjusted to match those in data.

To save computing time, we follow a two-step procedure to extract the ATGCs. We first use the GEANT-based D0 event simulation of diboson processes, reweighted with a SM NLO model of diboson production to produce a baseline sample of simulated events for comparison with data. We then use a simulation with ATGCs to create a set of predictions relative to the SM, $R \propto \sigma/\sigma_{SM}$. The ratio R is used to reweight the SM GEANT-based simulation to reflect ATGCs. This reweighted simulation is then compared to data and used to extract possible values of the ATGCs.

The effect of ATGCs is to increase the production cross section, especially at high boson transverse momentum, relative to its SM prediction. We therefore use the corresponding p_T^{jj} and $p_T^{\ell\ell}$ distributions to set the limits on ATGCs. The SM p_T^{jj} and $p_T^{\ell\ell}$ distributions are reweighted with R at the parton level. The reweighting method uses the ratio of matrix element squared values with and without the ATGC component to predict a change of the SM event rate in the presence of ATGCs. The basis of the reweighting method is that the equation of the differential cross section, which has a quadratic dependence on the anomalous couplings, can be written as:

$$
\begin{aligned}
d\sigma &\propto |\mathcal{M}|^2 \, dx \\
&\propto |\mathcal{M}|^2_{SM} \frac{|\mathcal{M}|^2}{|\mathcal{M}|^2_{SM}} \, dx \\
&\propto |\mathcal{M}|^2_{SM} \big[1 + A\Delta\kappa + B(\Delta\kappa)^2 + C\lambda + D\lambda^2 + E\Delta\kappa\lambda + \cdots\big] \, dx \\
&\propto d\sigma_{SM} \cdot R(\Delta\kappa, \lambda, \ldots),
\end{aligned}
\tag{5}
$$

where $d\sigma$ is the differential cross section that includes the contribution from the ATGCs; $d\sigma_{SM}$ is the SM differential cross section; $|\mathcal{M}|^2$ is the matrix element squared in the presence of ATGCs; $|\mathcal{M}|^2_{SM}$ is the matrix element squared in the SM; A, B, C, D, E, etc. are reweighting coefficients; and x is a kinematic variable sensitive to ATGCs.

In the LEP parametrization, Eq. (5) is parametrized with the three couplings $\Delta\kappa_\gamma$, λ, and Δg_1^Z and nine reweighting coefficients, A–I. Thus, the weight R in the LEP parametrization scenario is defined as:

$$
\begin{aligned}
R(&\Delta\kappa_\gamma, \lambda, \Delta g_1) \\
&= 1 + A\Delta\kappa_\gamma + B(\Delta\kappa_\gamma)^2 + C\lambda + D\lambda^2 + E\Delta g_1 \\
&\quad + F(\Delta g_1)^2 + G\Delta\kappa_\gamma\lambda + H\Delta\kappa_\gamma\Delta g_1 + I\lambda\Delta g_1,
\end{aligned}
\tag{6}
$$

with $\lambda = \lambda_\gamma = \lambda_Z$ and $\Delta g_1 = \Delta g_1^Z$.

In the equal couplings scenario, Eq. (5) is parametrized with the two couplings $\Delta\kappa$ and λ and five reweighting coefficients, A–E. In this case the weight is defined as:

$$
R(\Delta\kappa, \lambda) = 1 + A\Delta\kappa + B(\Delta\kappa)^2 + C\lambda + D\lambda^2 + E\Delta\kappa\lambda,
\tag{7}
$$

with $\Delta\kappa = \Delta\kappa_\gamma = \Delta\kappa_Z$ and $\lambda = \lambda_\gamma = \lambda_Z$. Depending on the number of reweighting coefficients, a system of the same number of equations allows us to calculate their values for each event. Then for any ATGC combination we can calculate R and apply it to the SM distribution to describe that kinematic distribution in the presence of the chosen non-SM TGC. We first calculate R_i ($i = 1$–5 for the equal couplings scenario and $i = 1$–9 for the LEP parameterization) with a fixed set of ATGCs using a LO prediction from the MCFM generator (with CTEQ6L1 PDFs). Therefore each MCFM event is assigned a value of $|\mathcal{M}|^2_{SM}$ and a set of $|\mathcal{M}|^2$ values for $\Delta\kappa_\gamma = \pm 1$, $\lambda = \pm 1$, $\Delta g_1^Z = \pm 1$, $\Delta\kappa_\gamma\lambda = +1$, $\Delta\kappa_\gamma\Delta g_1^Z = +1$, and $\lambda\Delta g_1^Z = +1$. For every bin X in the multidimensional phase space defined by different kinematic distributions, the ratio R is calculated as:

$$
R_{i;X} = \frac{\sum_j |\mathcal{M}_{i,j}|^2_X}{\sum_j |\mathcal{M}^{SM}_{i,j}|^2_X},
\tag{8}
$$

where j indicates the event number in bin X, and i is any of nine (five) ATGC combinations in the LEP parameterization (equal couplings scenario). The multidimensional phase space for the $WW \to \ell\nu jj$ events is defined by a set of kinematic variables at generator level, namely the transverse momentum (p_T) of the $q\bar{q}$ system, $p_T^{q\bar{q}}$, p_T of the leading parton, p_T of the trailing parton, p_T of the neutrino, p_T of the charged lepton, and the invariant mass of the $q\bar{q}$ system. For $WZ \to \ell\nu jj$ events, we use the p_T distribution of the quark, the p_T distribution of the anti-quark, $p_T^{q\bar{q}}$, p_T of the neutrino, p_T of the charged lepton, and the invariant mass of the $q\bar{q}$ system. For $WZ \to \ell\nu\ell\ell$ events, X is defined by the transverse momentum of the dilepton system, $p_T^{\ell\ell}$, where both leptons originate from the Z boson, p_T of the leading and the trailing leptons originating from the Z boson, p_T of the lepton originating from the W boson, and p_T of the neutrino.

When searching for ATGCs in the LEP parametrization, we vary two of the three couplings at a time, leaving the third coupling fixed to its SM value. This gives the three two-parameter combinations $(\Delta\kappa_\gamma, \lambda)$, $(\Delta\kappa_\gamma, \Delta g_1^Z)$, and $(\lambda, \Delta g_1^Z)$. For the equal couplings scenario there is only the $(\Delta\kappa, \lambda)$ combination. For a given pair of ATGC values, each SM event is weighted at the generator level by the appropriate weight $R_{i;X}$ and all the weights in a reconstructed p_T^{jj} (or $p_T^{\ell\ell}$) bin are summed. Such reweighted SM distributions are compared to data to determine which ATGCs are most consistent with observation. Kinematic distributions in $W\gamma \to \ell\nu\gamma$ and $WW \to \ell\nu\ell\nu$ production sensitive to ATGCs are the E_T of the photon, E_T^γ, and p_T distributions of the two leptons, respectively. The effects of ATGCs on the E_T^γ distribution are modeled using simulated events from the BHO generator [31] which undergo GEANT-based D0 detector simulation. In case of $\ell\nu\ell\nu$ final states, the ATGCs effects on p_T distributions of the two leptons are simulated using the HWZ generator [2] and passed through a parameterized simulation of the D0 detector that is tuned to data.

In order to verify the derived reweighting parameters, we calculate the weights $R_{i;X}$ for different $\Delta\kappa$, λ, and/or Δg_1^Z values, apply the reweighting coefficients and compare reweighted p_T shapes at the generator level to those predicted by MCFM. This procedure is also repeated after applying generator level selection cuts similar to those at the reconstructed level to check that the (acceptance $\times$ efficiency) for reconstructed events is reasonably modeled by this reweighting method. The agreement in the shape and normalization of the $p_T^{q\bar{q}}$ and $p_T^{\ell\ell}$ distributions used for the ATGC measurement is within 5% of the MCFM predictions and thus a conservative systematic uncertainty of 5% has been assigned to the reweighting method.
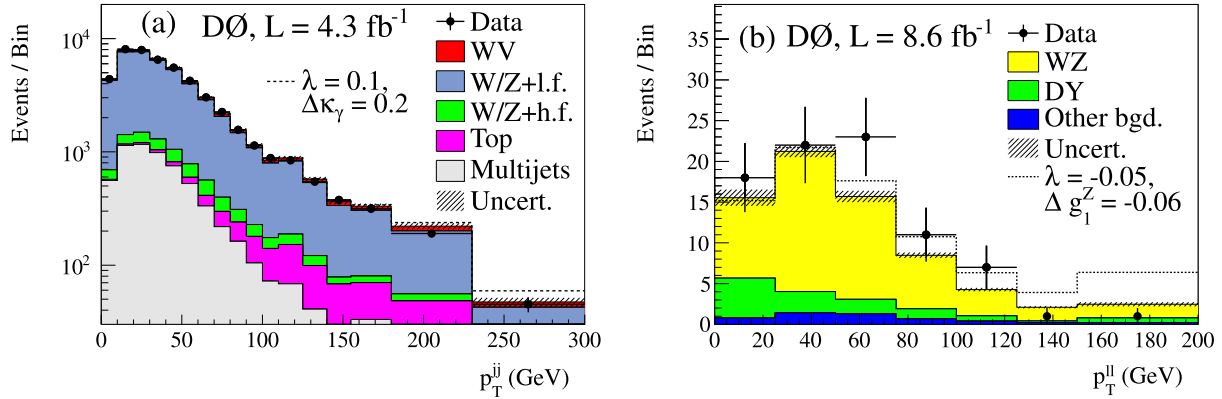
Fig. 1. (Color online.) (a) The p_T^{jj} distribution summed over electron and muon channels from $WW + WZ \to \ell\nu jj$ ($l = \mu, e$) production for data and SM MC predictions ("l.f." denotes light partons such as u, d, s or gluon, and "h.f." denotes heavy-flavor such as c or b). Also shown are expected distributions for an ATGC model with $\Delta\kappa_\gamma = 0.2$, and $\lambda = 0.1$. (b) The p_T^{ll} distribution summed over eee, $e\mu\mu$, μee and $\mu\mu\mu$ channels from $WZ \to \ell\nu\ell\ell$ production for data, SM MC predictions and for ATGC model with $\lambda = -0.05$ and $\Delta g_1^Z = -0.06$.
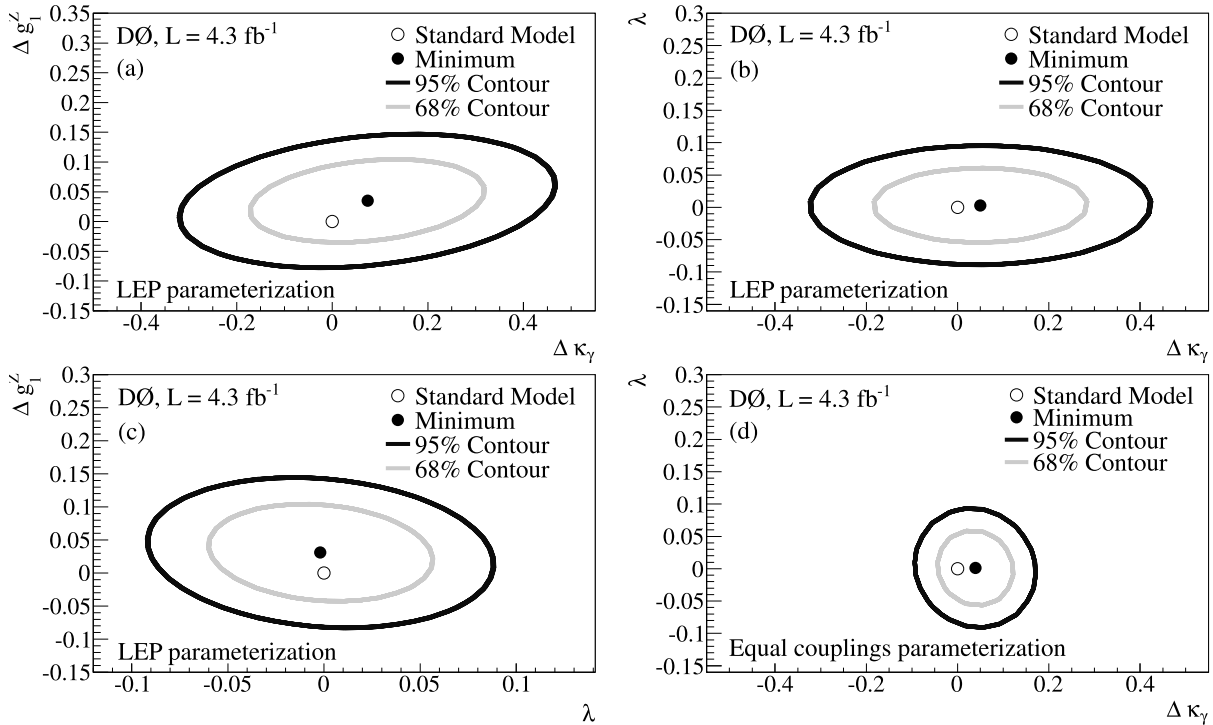
Fig. 2. $WW + WZ \to \ell\nu jj$ ($l = \mu, e$). The 68% and 95% C.L. two-parameter limits on the $\gamma WW/ZWW$ coupling parameters assuming the LEP (a), (b), (c) and equal couplings parameterization (d) with $\Lambda = 2$ TeV. Black circles indicate the most probable values of ATGCs from the two-parameter fit.

In the ATGC analysis of $\ell\nu jj$ final states, we consider two classes of systematic uncertainties: those related to the overall normalization and efficiencies of the various contributing physical processes, and uncertainties that, when propagated through the analysis, impact the shape of the dijet p_T distribution. We determine the dependence of the dijet p_T distribution on these uncertainties by varying each parameter by its uncertainty (± 1 standard deviation) and re-evaluating the shape of the dijet p_T distribution. The uncertainties with the largest impact are those related to background cross sections (6.3–20%), integrated luminosity (6.1%), the jet energy scale (3–9%) and the jet energy resolution (1–10%) although the analysis of the $\ell\nu jj$ final states is fully dominated by statistical uncertainty. In the analysis of $\ell\nu\ell\ell$ final states the most important systematic uncertainties arise from the diboson p_T modeling (0.1–0.4%), the lepton/jet energy scale (0.2–6.0%), and the

mis-modeling of lepton/jet resolution (1%). However, the systematic uncertainties are negligible compared to statistical uncertainties. Similarly, the $\ell\nu\ell\nu$ final states are mainly affected by statistical uncertainty while the systematic uncertainties arise from the background modeling ($< 7\%$), integrated luminosity (6.1%), lepton identification and trigger efficiencies ($< 3\%$). In the analysis of $\ell\nu\gamma$ final states systematic uncertainties due to integrated luminosity (6.1%), lepton and photon identification (1–5%), background modeling (1–10%) and theoretical predictions on the production cross sections (3–6%) dominate the total uncertainty.

The limits are determined from a fit of SM and ATGC contributions to the data using the reconstructed variables: the p_T^{jj} distribution from $WW + WZ \to \ell\nu jj$ production, the $p_T^{\ell\ell}$ distribution from $WZ \to \ell\nu\ell\ell$ production, the E_T^γ distribution from $W\gamma \to \ell\nu\gamma$ production, and the p_T distributions of the two

Table 1
The 95% C.L. one-parameter limits on ATGCs from $WZ \to \ell\nu\ell\ell$ and $WW + WZ \to \ell\nu jj$ ($l = \mu, e$) final states with $\Lambda = 2$ TeV. The analyzed integrated luminosity for each analysis is also presented together with the time period of data collection.

LEP parametrization	Integrated luminosity	$\Delta\kappa_\gamma$	λ	Δg_1^Z
$WZ \to \ell\nu\ell\ell$	8.6 fb^{-1} (2002–2011)	–	$[-0.077, 0.089]$	$[-0.055, 0.117]$
$WW + WZ \to \ell\nu jj$	4.3 fb^{-1} (2006–2009)	$[-0.27, 0.37]$	$[-0.075, 0.080]$	$[-0.071, 0.137]$

Equal couplings parametrization	Integrated luminosity	$\Delta\kappa$		λ
$WZ \to \ell\nu\ell\ell$	8.6 fb^{-1} (2002–2011)	–		$[-0.077, 0.090]$
$WW + WZ \to \ell\nu jj$	4.3 fb^{-1} (2006–2009)	$[-0.078, 0.153]$		$[-0.074, 0.079]$
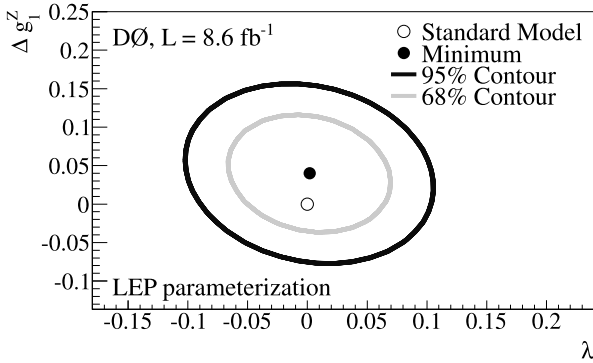
Fig. 3. $WZ \to \ell\nu\ell\ell$ ($l = \mu, e$). The 68% and 95% C.L. two-parameter limits on the $\gamma WW / ZWW$ coupling parameters assuming the LEP parametrization with $\Lambda = 2$ TeV. The black circle indicates the most probable values of ATGCs from the two-parameter fit.

Table 2
One-dimensional χ^2 minimum and 68% and 95% C.L. allowed intervals on anomalous values of $\gamma WW / ZWW$ ATGCs from the combined fit of $WW + WZ \to \ell\nu jj$, $WZ \to \ell\nu\ell\ell$, $W\gamma \to \ell\nu\gamma$, and $WW \to \ell\nu\ell\nu$ final states.

Results for LEP parameterization Parameter	Minimum	68% C.L.	95% C.L.
$\Delta\kappa_\gamma$	0.048	$[-0.057, 0.154]$	$[-0.158, 0.255]$
Δg_1^Z	0.022	$[-0.008, 0.054]$	$[-0.034, 0.084]$
λ	0.007	$[-0.015, 0.028]$	$[-0.036, 0.044]$
μ_W ($e/2M_W$)	2.012	$[1.978, 2.047]$	$[1.944, 2.080]$
q_W (e/M_W^2)	-0.995	$[-1.038, -0.953]$	$[-1.079, -0.916]$

Results for Equal couplings parameterization Parameter	Minimum	68% C.L.	95% C.L.
$\Delta\kappa$	0.037	$[-0.007, 0.081]$	$[-0.049, 0.124]$
λ	0.008	$[-0.017, 0.028]$	$[-0.039, 0.042]$
μ_W ($e/2M_W$)	2.016	$[1.982, 2.050]$	$[1.948, 2.082]$
q_W (e/M_W^2)	-1.009	$[-1.050, -0.970]$	$[-1.092, -0.935]$

leptons from $WW \to \ell\nu\ell\nu$ production. The p_T^{jj} and $p_T^{\ell\ell}$ distributions from 4.3 fb^{-1} and 8.6 fb^{-1} analyses, respectively, are shown in Fig. 1. The E_T^γ and lepton's p_T distributions, and the p_T^{jj} distribution from 1.1 fb^{-1} analysis can be found elsewhere [14–17]. The individual contributions are fit to the data as in the presence of ATGCs by minimizing the χ^2 function with respect to Gaussian priors on each of the systematic uncertainties [32]. The fit is performed simultaneously on kinematic distributions corresponding to the different sub-channels and data epochs. The remaining p_T^{jj} distributions for the electron and muon channels from the 1.1 fb^{-1} $WW + WZ \to \ell\nu jj$ analysis are fit separately and the χ^2 values are summed with those obtained in the simultaneous fit. The effects of systematic uncertainties on separate samples and sub-channels due to the same uncertainty are assumed to be 100% correlated but different uncertainties are assumed to be uncorrelated.

The 68% and 95% C.L. limits on ATGCs from the 4.3 fb^{-1} analysis of $WW + WZ \to \ell\nu jj$ final states in the two-parameter space are shown in Fig. 2. The limits from the 8.6 fb^{-1} analysis of $WZ \to \ell\nu\ell\ell$ final states are presented only in the $\lambda - \Delta g_1^Z$ space as shown in Fig. 3, because WZ production is weakly sensitive to $\Delta\kappa_\gamma$ via the relation given by Eq. (3). The 95% C.L. one-parameter limits, obtained from single parameter fits with all other parameters fixed to their SM values are presented in Table 1.

The resulting 68% and 95% C.L. one-parameter limits from the combined fit of $\ell\nu\gamma$, $\ell\nu\ell\nu$, $\ell\nu jj$, and $\ell\nu\ell\ell$ final states are shown in Table 2 and limits in two-parameter space are shown in Fig. 4. The limits in both scenarios represent an improvement relative to previous results from the Tevatron [6,7,14–17]. For the LEP parametrization, our combined measurement with 68% C.L. allowed intervals of $\kappa_\gamma = 1.048^{+0.106}_{-0.105}$, $\lambda = 0.007^{+0.021}_{-0.022}$, and $g_1^Z = 1.022^{+0.032}_{-0.030}$ presented in this Letter has similar sensitivity to the results from the individual LEP experiments [8–11]. The combined D0 limits are more stringent than those set by the ATLAS Col-

laboration for $\Lambda = 2$ TeV [12]. The limits from the CMS Collaboration [13] are not directly comparable to our results due to a different assumption for Λ value that affects a dipole form factor and thus, the sensitivity to ATGCs [33]. Nevertheless, the combined D0 limits on $\Delta\kappa_\gamma$, λ and Δg_1^Z are more stringent than both ATLAS and CMS current limits for $\Lambda \to \infty$.

Using observed limits we extract measurements of the W boson magnetic dipole and electric quadrupole moments. When assuming the LEP parameterization with $g_1^Z = 1$, we set the 68% C.L. intervals of $\mu_W = 2.012^{+0.035}_{-0.034}$ ($e/2M_W$) and $q_W = -0.995^{+0.042}_{-0.043}$ (e/M_W^2). The 68% and 95% C.L. limits on μ_W and q_W in both scenarios are shown in Fig. 5.

In summary, we have presented new searches of anomalous γWW and ZWW trilinear gauge boson couplings from $WW + WZ \to \ell\nu jj$ and $WZ \to \ell\nu\ell\ell$ channels analyzing 4.3 fb^{-1} and 8.6 fb^{-1} of integrated luminosity, respectively, and we set limits on ATGCs for these final states. The limits from 4.3 fb^{-1} $\ell\nu jj$ analysis are the best limits to date at a hadron collider in this final state. The limits from 8.6 fb^{-1} $\ell\nu\ell\ell$ analysis are comparable to those set at the LHC and improve relative to previous limits set in this final state at the Tevatron [34]. We have combined these results with those previously published from $WW + WZ \to \ell\nu jj$ (1.1 fb^{-1}), $W\gamma \to \ell\nu\gamma$ (4.9 fb^{-1}), and $WW \to \ell\nu\ell\nu$ (1.0 fb^{-1}) final states using up to 8.6 fb^{-1} of integrated luminosity. No deviation from the SM is found in data. We set the most stringent limits on $\Delta\kappa_\gamma$, λ and Δg_1^Z at a hadron collider to date complementing similar measurements performed at LEP and LHC. Using the LEP parameterization we set the combined 68% C.L. limits of $-0.057 < \Delta\kappa_\gamma < 0.154$, $-0.015 < \lambda < 0.028$, and $-0.008 < \Delta g_1^Z < 0.054$. At 95% C.L. the limits are $-0.158 < \Delta\kappa_\gamma < 0.255$, $-0.036 < \lambda < 0.044$, and $-0.034 < \Delta g_1^Z < 0.084$. Based on the combination of all diboson production and decay channels we set the most stringent 68% C.L. constraints on the W boson magnetic dipole and electric quadrupole moments of $\mu_W = 2.012^{+0.035}_{-0.034}$ ($e/2M_W$) and $q_W = -0.995^{+0.042}_{-0.043}$ (e/M_W^2), respectively, to date.
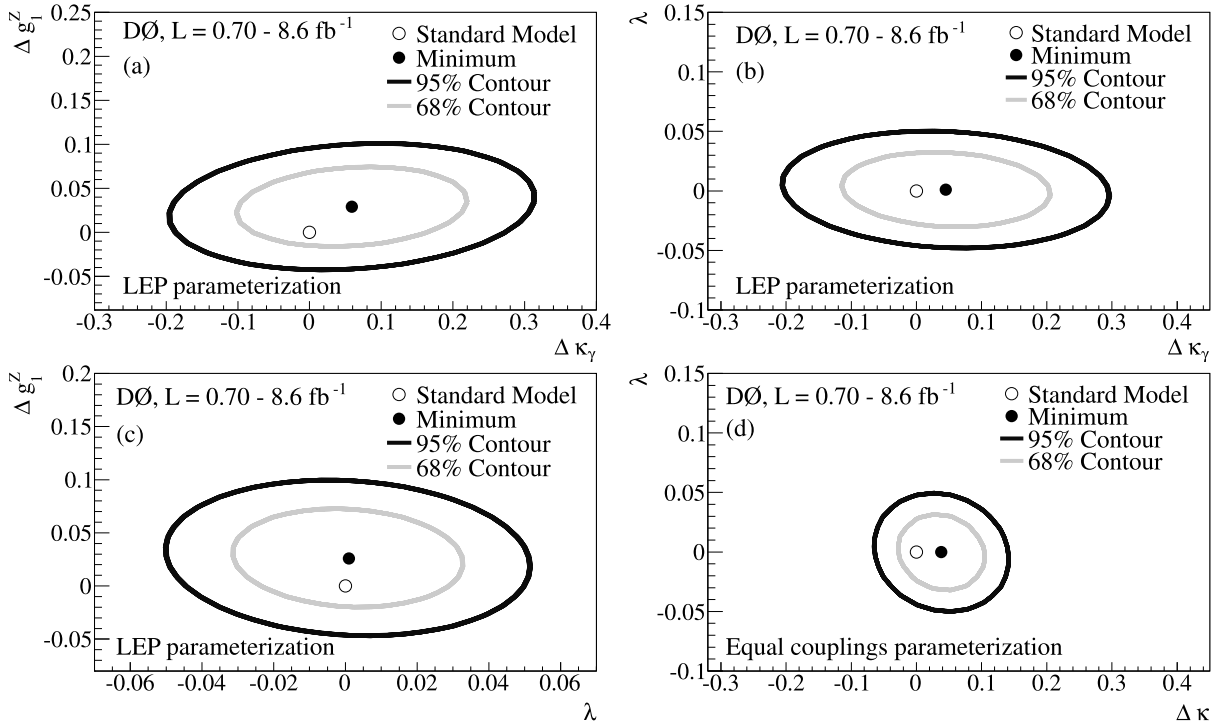
Fig. 4. The 68% and 95% C.L. two-parameter limits on the $\gamma WW / ZWW$ ATGCs $\Delta\kappa_\gamma$, $\Delta\lambda_\gamma$ and Δg_1^Z, assuming the LEP parametrization (a), (b), (c) and on $\Delta\kappa$ and λ ATGCs for the equal couplings parameterization (d) with $\Lambda = 2$ TeV from the combination of $WW + WZ \to \ell\nu jj$, $WZ \to \ell\nu\ell\ell$, $W\gamma \to \ell\nu\gamma$, and $WW \to \ell\nu\ell\nu$ final states ($l = \mu, e$). Black circles indicate the most probable values of ATGCs from the two-parameter fit.
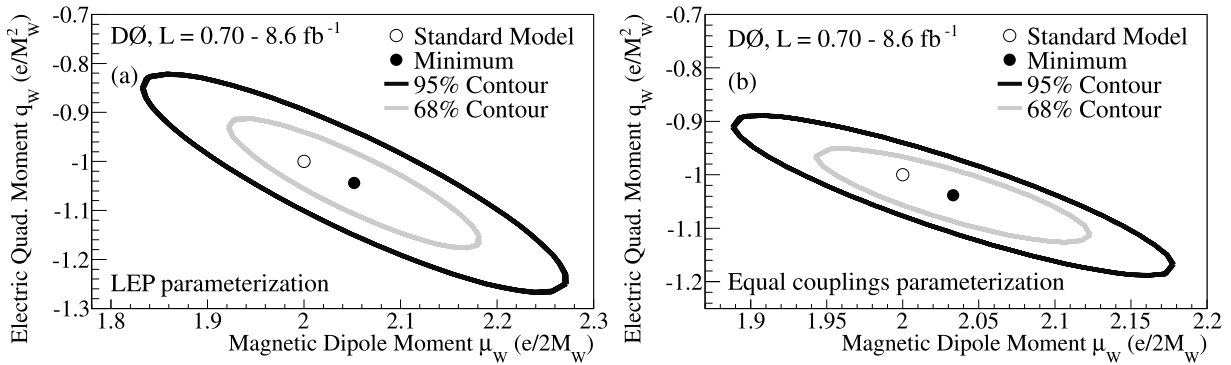
Fig. 5. Two-dimensional 68% and 95% C.L. limits for the W boson electric quadrupole moment vs. the magnetic dipole moment for (a) LEP parametrization and (b) equal couplings constraints from the combination of $WW + WZ \to \ell\nu jj$, $WZ \to \ell\nu\ell\ell$, $W\gamma \to \ell\nu\gamma$, and $WW \to \ell\nu\ell\nu$ final states ($l = \mu, e$). In both cases we assume $\Lambda = 2$ TeV. Black circles indicate the most probable values of μ_W and q_W from the two-parameter fit.

Acknowledgements

References

[1] K. Hagiwara, R.D. Peccei, D. Zeppenfeld, Nucl. Phys. B 282 (1987) 253.

[2] K. Hagiwara, J. Woodside, D. Zeppenfeld, Phys. Rev. D 41 (1990) 2113.
[3] S. Weinberg, Phys. Rev. D 13 (1976) 974;
L. Susskind, Phys. Rev. D 20 (1979) 2619;
H.P. Nilles, Phys. Rep. 110 (1984) 1;
H.E. Haber, G.L. Kane, Phys. Rep. 117 (1985) 75;
A.G. Cohen, D.B. Kaplan, A.E. Nelson, Phys. Lett. B 388 (1996) 588;
C. Csaki, C. Grojean, L. Pilo, J. Terning, Phys. Rev. Lett. 92 (2004) 101802;
R. Foadi, S. Gopalakrishna, C. Schmidt, J. High Energy Phys. 0403 (2004) 042.
[4] C. Grosse-Knetter, I. Kuss, D. Schildknecht, Z. Phys. C 60 (1993) 375;
M. Bilenky, J.L. Kneur, F.M. Renard, D. Schildknecht, Nucl. Phys. B 409 (1993) 22;
M. Bilenky, J.L. Kneur, F.M. Renard, D. Schildknecht, Nucl. Phys. B 419 (1994) 240.
[5] S. Alam, S. Dawson, R. Szalapski, Phys. Rev. D 57 (1998) 1577.
[6] B. Abbott, et al., D0 Collaboration, Phys. Rev. D 60 (1999) 072002.
[7] T. Aaltonen, et al., CDF Collaboration, Phys. Rev. D 76 (2007) 111103(R).
[8] S. Schael, et al., ALEPH Collaboration, Phys. Lett. B 614 (2005) 7.
[9] G. Abbiendi, et al., OPAL Collaboration, Eur. Phys. J. C 33 (2004) 463.
[10] P. Achard, et al., L3 Collaboration, Phys. Lett. B 586 (2004) 151.

[11] J. Abdallah, et al., DELPHI Collaboration, Eur. Phys. J. C 66 (2010) 35.
[12] G. Aad, et al., ATLAS Collaboration, Phys. Lett. B 712 (2012) 289;
G. Aad, et al., ATLAS Collaboration, Phys. Lett. B 717 (2012) 49;
G. Aad, et al., ATLAS Collaboration, http://dx.doi.org/10.1140/epjc/s10052-012-2173-0.
[13] S. Chatrchyan, et al., CMS Collaboration, Phys. Lett. B 701 (2011) 535.
[14] V.M. Abazov, et al., D0 Collaboration, Phys. Rev. Lett. 100 (2008) 241805.
[15] V.M. Abazov, et al., D0 Collaboration, Phys. Rev. Lett. 107 (2011) 241803.
[16] V.M. Abazov, et al., D0 Collaboration, Phys. Rev. Lett. 103 (2009) 191801.
[17] V.M. Abazov, et al., D0 Collaboration, Phys. Rev. D 80 (2009) 053012.
[18] V.M. Abazov, et al., D0 Collaboration, Nucl. Instrum. Methods Phys. Res. A 565 (2006) 463;
M. Abolins, et al., Nucl. Instrum. Methods A 584 (2007) 75;
R. Angstadt, et al., Nucl. Instrum. Methods Phys. Res. A 622 (2010) 298.
[19] S. Abachi, et al., D0 Collaboration, Nucl. Instrum. Methods Phys. Res. A 338 (1994) 185.
[20] V.M. Abazov, et al., D0 Collaboration, Nucl. Instrum. Methods Phys. Res. A 552 (2005) 372.
[21] V.M. Abazov, et al., D0 Collaboration, Phys. Rev. Lett. 108 (2012) 181803.
[22] V.M. Abazov, et al., D0 Collaboration, Phys. Rev. D 85 (2012) 112005.
[23] J. Smith, W.L. van Neerven, J.A.M. Vermaseren, Phys. Rev. Lett. 50 (1983) 1738.
[24] T. Sjöstrand, S. Mrenna, P. Skands, J. High Energy Phys. 0605 (2006) 026, version 6.409 is used.
[25] J. Pumplin, et al., J. High Energy Phys. 0207 (2002) 12;
J. Pumplin, et al., J. High Energy Phys. 0310 (2003) 46.
[26] S. Frixione, B.R. Webber, J. High Energy Phys. 0206 (2002) 029;
S. Frixione, P. Nason, B.R. Webber, J. High Energy Phys. 0308 (2003) 007, version 3.3 is used.
[27] G. Corcella, et al., J. High Energy Phys. 0101 (2001) 010.
[28] J. Campbell, R. Ellis, C. Williams, J. High Energy Phys. 1107 (2011) 018, we use mcfm version 6.0.
[29] P. Nason, J. High Energy Phys. 0411 (2004) 040;
S. Frixione, P. Nason, C. Oleari, J. High Energy Phys. 0711 (2007) 070.
[30] R. Brun, F. Carminati, CERN Program Library Long Writeup W5013 (1993).
[31] U. Baur, T. Han, J. Ohnemus, Phys. Rev. D 48 (1993) 5140.
[32] W. Fisher, FERMILAB-TM-2386-E, 2007.
[33] U. Baur, D. Zeppenfeld, Phys. Lett. B 201 (1988) 383.
[34] T. Aaltonen, et al., CDF Collaboration, http://dx.doi.org/10.1103/PhysRevD.86.031104;
V.M. Abazov, et al., D0 Collaboration, Phys. Lett. B 695 (2011) 67.